Structural Engineering and Mechanics, Vol. 5, No. 6 (1997) 853-865
DOI: http://dx.doi.org/10.12989/sem.1997.5.6.853

A field-consistency approach to plate elements

Gangan Prathap †

National Aerospace Laboratories, Bangalore 560-017, India
and Jawaharlal Nehru Centre for Advanced Scientific Research, Jakkur, Bangalore 560-064, India

Abstract. The design of robust plate and shell elements has been a very challenging area for several decades. The main difficulty has been the shear locking phenomenon in plate elements and the shear and membrane locking phenomena together in the shell elements. Among the various artifices or devices which are used to develop elements free of these problems is the field-consistency approach. In this paper this approach is reviewed. It turns out that not only Mindlin type elements but also elements based on higher-order theories could be developed using the technique.

Key words: plate elements; shear locking; field-consistency

1. Introduction

The design of a robust plate/shell element based on the Mindlin plate theory (Mindlin 1951), especially the 4-node quadrilateral, the work-horse QUAD4 element of all general purpose programs has been one of the most challenging tasks faced by element designers. The main difficulty was in understanding the shear locking phenomenon and eliminating it without producing other deleterious side-effects. Shear locking was first observed, not in the formulation of a plate element *ab initio* from a shear flexible plate theory such as the Mindlin plate theory but from the attempt to represent the behaviour of shells using what is called the degenerate shell approach (Ahmad, Irons and Zienkiewicz 1970). In this the shell behaviour is modelled directly after a slight modification of the 3D equations and shell geometry and domain are represented by a 3D brick element but its degrees of freedom are condensed to three displacements and two section rotations at each node. Unlike classical plate or shell theory, the transverse shear strain and its energy is therefore accounted for in this formulation. These elements behaved very poorly in representing even the trivial example of a plate in bending and the errors progressed without limit as the plates became thinner.

When the locking phenomenon was first encountered, the remedy proposed at once was the reduced integration of the shear strain energy (Zienkiewicz, Taylor and Too 1971, Pawsey and Clough 1971). This was only partially successful and many issues remained unresolved. Some of these were,

1) the 2×2 rule recommended in Zienkiewicz, Taylor and Too (1971) failed to remove shear locking in the 8-node serendipity plate element,
2) the 2×2 rule in the 9-node Lagrangian element removed locking but introduced spurious zero energy modes,

† Deputing Director

3) the selective 2×3 and 3×2 rule for the transverse shear strain energies from γ_{xz} and γ_{yz} recommended for a 8-node element in Pawsey and Clough (1971) also failed to remove shear locking,
4) the same selective 2×3 and 3×2 rule when applied to a 9 noded element is optimal for a rectangular form of the element but not when the element was distorted into a general quadrilateral form,
5) even after reduced integration of the shear energy terms, the degenerate shell elements performed poorly when trying to represent the bending of curved shells, due to an additional factor, identified as membrane locking (Stolarski and Belytschko 1982), originating now from the need for consistency of the membrane strain interpolations.

It was not possible to generalise the reduced integration rules for higher precision elements (8-node, 9-node, etc.) and it seemed impossible to derive a robust general quadrilateral using reduced integration only. Many methods now exist which make it possible to design robust elements. In this paper, we review the field-consistency approach which we believe offers a scientific paradigmatic basis (Prathap 1993).

2. Shear locking and field-consistency

It is useful now to review the shear locking phenomenon and the field-consistency explanation using the linear Timoshenko beam element as an example. An element based on elementary theory needs two nodes with 2 degrees of freedom at each node, the transverse deflection w and slope dw/dx and uses cubic interpolation functions to meet the C^1 continuity requirements of this theory (Fig. 1). A similar two-noded beam element based on the shear flexible Timoshenko beam theory will need only C^0 continuity and can be based on simple linear interpolations. It was therefore very attractive for general purpose applications. However, the element was beset with problems, as we shall presently see.

2.1. The conventional formulation of the linear beam element

The strain energy of a Timoshenko beam element of length $2l$ can be written as the sum of its bending and shear components as

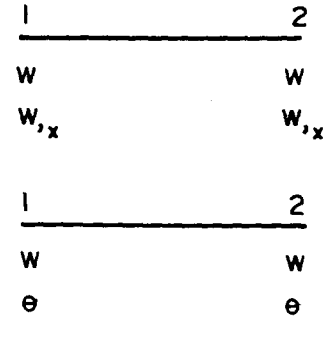

Fig. 1 Classical and Timoshenko beam element.

Table 1 Normalised tip deflections

No. of elements	"Thin" beam
1	0.200×10^{-4}
2	0.800×10^{-4}
4	0.320×10^{-3}
8	0.128×10^{-3}
10	0.512×10^{-3}

$$\int (1/2\ EI\ \kappa^T\ \kappa+1/2\ kGA\ \gamma^T\gamma)\ dx \tag{1}$$

where

$$\kappa=\theta_{,x} \tag{2a}$$

$$\gamma=\theta-w_{,x} \tag{2b}$$

In Eqs. (2a) and (2b), w is the transverse displacement and θ the section rotation. E and G are the Young's and shear moduli and k the shear correction factor used in Timoshenko's theory. I and A are the moment of inertia and the area of cross-section, respectively.

In the conventional procedure, linear interpolations are chosen for the displacement field variables as,

$$N_1=(1-\xi)/2 \tag{3a}$$

$$N_2=(1+\xi)/2 \tag{3b}$$

where the dimensionless coordinate $\xi=x/l$ varies from -1 to $+1$ for an element of length $2l$. This ensures that the element is capable of strain free rigid body motion and can recover a constant state of strain (completeness requirement) and that the displacements are continuous within the element and across the element boundaries (continuity requirement). We can compute the bending and shear strains directly from these interpolations using the strain gradient operators given in Eqs. (2a) and (2b). These are then introduced into the strain energy computation in Eq. (1), and the element stiffness matrix is calculated in an analytically or numerically exact (a 2 point Gauss Legendre integration rule) way.

We shall now model a cantilever beam under a tip load using this element, considering the case of a "thin" beam with $E=1000$, $G=37500000$, $t=1$, $L=4$, using a fictitiously large value of G to simulate the "thin" beam condition (Hughes, Taylor and Kanok-Nukulchai 1977). Table 1 shows that the normalized tip displacements are dramatically in error. In fact with a classical beam element model, exact answers would have been obtained with one element for this case. We can carefully examine Table 1 to see the trend as the number of elements is increased. The tip deflections obtained, which are several orders of magnitude lower than the correct answer, are directly related to the square of the number of elements used for the idealization. In other words, the resulting answer has a stiffness related to the inverse of N^2. This is clearly unrelated to the physics of the Timoshenko beam and also not the usual sort of discretization errors encountered in the finite element method. It is this very phenomenon that is known as shear locking.

The error in each element must be related to the element length, and therefore when a beam

of overall length L is divided into N elements of equal length h, the additional stiffening introduced in each element due to shear locking is seen to be proportional to h^2. In fact, numerical experiments showed that the locking stiffness progresses without limit as the element depth t decreases. Thus, we now have to look for a mechanism that can explain how this spurious stiffness of $(h/t)^2$ can be accounted for by considering the mathematics of the discretization process.

The magic formula proposed to overcome this locking is the reduced integration method. The bending component of the strain energy of a Timoshenko beam element of length $2l$ shown in Eq. (1) is integrated with a one-point Gaussian rule as this is the minimum order of integration required for exact evaluation of this strain energy. However, a mathematically exact evaluation of the shear strain energy will demand a two-point Gaussian integration of the shear strain energy component causes the shear related stiffness matrix to change to lower rank. The performance of this element was extremely good, showing no signs of locking at all.

2.2. The field-consistency paradigm

It is clear from the formulation of the linear Timoshenko beam element using exact integration (we shall call it the field-inconsistent element) that ensuring the completeness and continuity conditions are not enough in some problems. We shall propose a requirement for a consistent interpolation of the constrained strain fields as the necessary paradigm to make our understanding of the phenomena complete.

If we start with linear trial functions for w and θ, as we had done in Eqs. (3) above, we can associate two generalized displacement constants with each of the interpolations in the following manner

$$w=\alpha_0+\alpha_1\ (x/l) \tag{4a}$$

$$\theta=b_0+b_1\ (x/l) \tag{4b}$$

We can relate such constants to the field-variables obtaining in this element in a discretized sense; thus, $\alpha_1/l=w_{,x}$ at $x=0$, $b_0=\theta$ and $b_1/l=\theta_{,x}$ at $x=0$.

If the strain-fields are now derived from the displacement fields given in Eqs. (4), we get

$$\kappa=(b_1/l) \tag{5a}$$

$$\gamma=(b_0-\alpha_1/l)+b_1(x/l) \tag{5b}$$

An exact evaluation of the strain energies for an element of length $h=2l$ will now yield the bending and shear strain energy as

$$U_B=1/2\ (EI)\ (2l)\ \{(b_1/l)\}^2 \tag{6a}$$

$$U_S=1/2\ (kGA)\ (2l)\ \{(b_0-\alpha_1/l)^2+1/3\ b_1^2\} \tag{6b}$$

It is possible to see from this that in the constraining physical limit of a very thin beam modelled by elements of length $2l$ and depth t, the shear strain energy in Eq. (6b) must vanish. An examination of the conditions produced by this requirement shows that the following constraints would emerge in such a limit

$$b_0-\alpha_1/l \rightarrow 0 \tag{7a}$$

$$b_1 \rightarrow 0 \tag{7b}$$

In our new terminology (Prathap 1993) constraint (7a) is field-consistent as it contains constants from both the contributing displacement interpolations relevant to the description of the shear strain field. These constraints can then accommodate the true Kirchhoff constraints in a physically meaningful way, i.e., in an infinitesimal sense, this is equal to the condition $(\theta - w_{,x}) \rightarrow 0$ at the element centroid. In direct contrast, constraint (6.7b) contains only a term from the section rotation θ. A constraint imposed on this will lead to an undesired restriction on θ. In an infinitesimal sense, this is equal to the condition $\theta_{,x} \rightarrow 0$ at the element centroid (i.e., no bending is allowed to develop in the element region). This is the 'spurious constraint' that leads to shear locking and violent disturbances in the shear force prediction over the element, as we shall see presently.

2.3. The consistent formulation of the linear element

We can see that reduced integration ensures that the inconsistent constraint does not appear and so is effective in producing a consistent element, at least in this instance. We must now satisfy ourselves that such a modification did not violate any variational theorem.

The field-consistent element, as we now shall call an element version free of spurious (i.e., inconsistent) constraints, can and has been formulated in various other ways as well. The 'trick' is to evaluate the shear strain energy, in this instance, in such a way that only the consistent term will contribute to the shear strain energy. Techniques like addition of bubble modes, hybrid methods etc. can produce the same results, but in all cases, the need for consistency of the constrained strain field must be absolutely met.

We explain now why the use of a trick like the reduced integration technique, or the use of assumed strain methods allows the locking problem to be overcome. It is obvious that it is not possible to reconcile this within the ambit of the minimum total potential principle only, which had been the starting point of the conventional formulation.

To eliminate problems such as locking, we look for a consistent constrained strain field to replace the inconsistent kinematically derived strain field in the minimum total potential principle. By closely examining the strain gradient operators it is possible to identify the order up to which the consistent strain field must be interpolated. In this case, for the linear displacement interpolations, Eqs. (5b), (7a) and (7b) tell us that the consistent interpolation should be a constant. At this point we shall still not presume what this constant should be, although past experience suggests it is the same constant term seen in Eq. (7a). Instead, we bring in the Hellinger-Reissner theorem in the following form to see the identity of the consistent strain field clearly. For now, it is sufficient to note that the Hellinger-Reissner theorem is a restricted case of the Hu-Washizu theorem. In this theorem, the functional is stated in the following form

$$\int (-1/2\ EI\ \bar{\kappa}^T\ \bar{\kappa} + EI\ \bar{\kappa}^T\ \kappa - 1/2\ kGA\ \bar{\gamma}^T\bar{\gamma} + kGA\ \bar{\gamma}^T\gamma)\ dx \tag{8}$$

where $\bar{\kappa}$ and $\bar{\gamma}$ are the new strain variables introduced into this multi-field principle. Since we have difficulty only with the kinematically derived γ we can have $\bar{\kappa}=\kappa$ and recommend the use of a $\bar{\gamma}$ which is of consistent order to replace γ. A variation of the functional in Eq. (8) with respect to the as yet undetermined coefficients in the interpolation for $\bar{\gamma}$ yields

$$\int \delta\bar{\gamma}^T\ (\bar{\gamma} - \gamma)\ dx = 0 \tag{9}$$

This orthogonality condition now offers a means to constitute the coefficients of the consistent strain field from the already known coefficients of the kinematically derived strain field. Thus, for γ given by Eq. (5b), it is possible to show that $\bar{\gamma}=(b_0-\alpha_1/l)$. In this simple instance, the same result is obtained by sampling the shear strain at the centroid, or by the use of one-point Gaussian integration. What is important is that, deriving the consistent strain-field using this orthogonality relation and then using this to compute the corresponding strain energy will yield a field-consistent element which does not violate any of the variational norms, i.e., an exact equivalence to the mixed element exists without having to go through the additional operations in a mixed or hybrid finite element formulation, at least in this simple instance. We say that the variational correctness of the procedure is assured (Prathap 1993). The substitute strain interpolations derived thus can therefore be easily coded in the form of strain function subroutines and used directly in the displacement type element stiffness derivations.

2.4. Some concluding remarks on the linear beam element

So far we have seen the linear beam element as an example to demonstrate the principles involved in the finite element modelling of a constrained media problem. We can demonstrate that a conceptual framework that includes a condition that specifies that the strain fields which are to be constrained must satisfy a consistency criterion is able to provide a complete scientific basis for the locking problems encountered in conventional displacement type modelling (Prathap 1993). We can also show that a correctness criterion (which links the assumed strain variation of the displacement type formulation to the mixed variational theorems) allows us to determine the consistent strain field interpolation in a unique and mathematically satisfying manner (Prathap 1993).

3. Rectangular four-node bi-linear plate bending element

Mindlin's approximations permit a simple description of plate behaviour. Only first order derivative terms appear in the strain-displacement relations-therefore compatible Mindlin elements require the fields w, θ_x and θ_y to be only C^0 continuous, where x, y are Cartesian co-ordinates, w is the transverse displacement, θ_x and θ_y are the section rotations, and hence low order shape functions suffice to represent these fields.

The 4-node rectangular bi-linear element is the simplest element based on Mindlin theory that could be devised. It was established (Hughes, Taylor and Kanok-Nukulchai 1997) that an exactly integrated Mindlin plate element would lock. Locking was seen to vanish for the rectangular element if a reduced 1-point Gauss integration rule was used for the shear strain energy. This rectangular element behaved very well if the plate was thin but the results deteriorated as the plate became thicker. Also, after distortion to a quadrilateral form, locking re-appeared. We can now demonstrate from our consistency view-point why the 1-point integration of the shear strain energy is inadequate to retain all the true Kirchhoff constraints in a thin plate element and also why such a strategy cannot preserve consistency if the element was distorted.

The strain energy for an isotropic, linear elastic plate element according to Mindlin theory is constituted from its bending and shear energies as

$$U=U_B+U_S$$
$$=\frac{Et^3}{24(1-\nu^2)}\left\{\int\int [\theta_{x,x}^2+\theta_{y,y}^2+2\nu\ \theta_{x,x}\theta_{y,y}+(1-\nu)/2\ (\theta_{x,y}+\theta_{y,x})^2]\ dx\ dy\right.$$
$$\left.+\frac{6k(1-\nu)}{t^2}\int\int [(\theta_x-w_{,x})^2+(\theta_y-w_{,y})^2]\ dx\ dy\right\} \tag{10}$$

where E is the Young's modulus, ν is the Poisson's ratio, k is the shear correction factor and t is the plate thickness. The factor k is introduced to compensate for the error in approximating the shear strain as a constant over the thickness direction of a Mindlin plate.

The bending energy causes no problem. It is the shear energies which must be looked at carefully. Let us now examine the field-consistency requirements for one of the shear strains, γ_{xz}, in the Cartesian system. The admissible displacement field interpolations required to describe this shear strain field can be written in terms of the Cartesian co-ordinates itself as

$$w=\alpha_0+\alpha_1 x+\alpha_2 y+\alpha_3 xy \tag{11a}$$
$$\theta=b_0+b_1 x+b_2 y+b_3 xy \tag{11b}$$

The shear strain field derived from these kinematically admissible shape functions is,

$$\gamma_{xz}=(b_0-\alpha_1)+(b_2-\alpha_3)y+b_1 x+b_3 xy \tag{12}$$

As the plate thickness is reduced to zero, the shear strains must vanish. The discretized constraints that are seen to be enforced as $\gamma_{xz}\rightarrow 0$ in Eq. (12) are

$$b_0-\alpha_1\rightarrow 0 \tag{13a}$$
$$b_2-\alpha_3\rightarrow 0 \tag{13b}$$
$$b_1\rightarrow 0 \tag{13c}$$
$$b_3\rightarrow 0 \tag{13d}$$

The constraints shown in Eqs. (13a) and (13b) are physically meaningful and represent the Kirchhoff condition in a discretized form. Constraints (13c) and (13d) are the cause for concern here-these are the spurious or 'inconsistent' constraints which lead to shear locking. Thus, in a rectangular element, the requirement for consistency of the interpolations for the shear strains in the Cartesian co-ordinate system is easily recognized as the polynomials use only Cartesian co-ordinates. Let us now try to derive the optimal element and also understand why the simple 1-point strategy led to zero energy mechanisms.

It is clear from Eqs. (12) and (13) that the terms $b_1 x$ and $b_3 xy$ are the inconsistent terms which will contribute to locking in the form of spurious constraints. We must now find an optimal integration strategy for removing shear locking without introducing any zero energy mechanisms. We shall consider first, the part of the shear strain energy contributed by γ_{xz}. An exact integration, that is a 2×2 Gaussian integration of the shear strain energy leads to the four constraint quantities seen in Eq. (13). The first two reproduce the true Kirchhoff constraints and the remaining two act as spurious constraints that cause shear locking by enforcing $\theta_{x,x}\rightarrow 0$ and $\theta_{x,xy}\rightarrow 0$ in the element.

If a 1×2 Gaussian integration is used only the true constraints are retained and all spurious constraints are removed.

By a very similar argument, we can show that the part of the shear strain energy from γ_{yz} will require a 2×1 Gaussian integration rule. This element would be the optimal rectangular bi-linear Mindlin plate element.

Let us now look at the 1-point integration strategy. This will give shear energy terms which reflect only one true constraint each for the shear energy from γ_{xz} and γ_{yz} respectively while th other Kirchhoff constraints $(\theta_x - w_{,x})_{,yo} \rightarrow 0$ and $(\theta_x - w_{,y})_{,xo} \rightarrow 0$ are lost. This introduces two zero energy modes and accounts for the consequent deterioration in performance of the element when the plates are thick or are very loosely constrained.

We have seen now that it is a very simple procedure to re-constitute field-consistent assumed strain fields from the kinematically derived fields such as shown in Eq. (12) so that they are also variationally correct. This is not so simple in a general quadrilateral where the complication arising from the isoparametric mapping from a natural co-ordinate system to a Cartesian system makes it very difficult to see the consistent form clearly. We shall see the difficulties associated with this form in the next section.

4. The four-node quadrilateral plate element

The Cartesian co-ordinate system is mapped from the natural co-ordinate system using the isoparametric shape functions and these are also used to interpolate the degrees of freedom w, θ_x and θ_y (Fig. 2). Note that the section rotations are described in the Cartesian system and this fact assumed a crucial importance when consistency of the shear strain definitions of an arbitrarily deformed quadrilateral are sought. Thus the geometry of the element and the displacement fields are now expressed in terms of the isoparametric 4-node shape functions as

$$(x,\ y,\ w,\ \theta_x,\ \theta_y) = \sum N_i^o(\xi,\ \eta)\ (x_i,\ y_i,\ w_i,\ \theta_{xi},\ \theta_{yi}) \tag{14}$$

where the subscript 'i' indicates the nodal values. The superscript 'o' is used to denote that

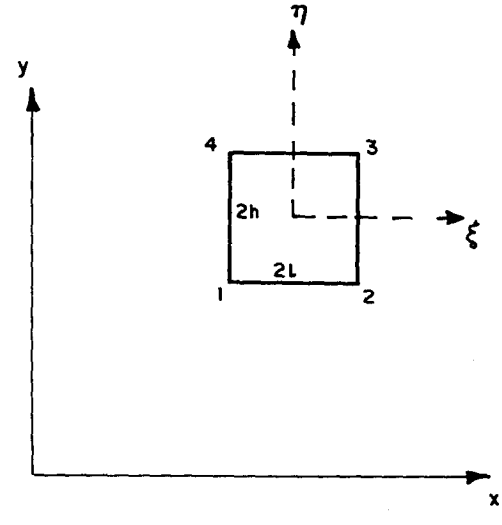

Fig. 2 Cartesian and natural coordinate system for a 4-noded φ rectangular plate element.

these are the original isoparametric shape functions. Later, we would have to derive substitute shape functions (or smoothed shape functions as they are sometimes called) for the sole purpose of achieving consistent shear strain interpolations and these we will separately designate using superscripts '1' etc. The usual bi-linear shape functions are used, where $N_i^o(\xi, \eta)=0.25\ (1+\xi\xi_i)(1+\eta\eta_i)$ and (ξ_i, η_i) are the local co-ordinates of the node i.

The Jacobian $[J]$ will play an important role in locating the special difficulties that originate in trying to define consistent expressions for shear strain for a quadrilateral element. The elements of this matrix (α_{ij} of $[J]$), and its inverse (b_{ij} of $[J]^{-1}$), are obtained as: $\alpha_{11}=x_{,\xi}$, $\alpha_{12}=y_{,\xi}$, $\alpha_{21}=x_{,\eta}$, $\alpha_{22}=y_{,\eta}$, and $b_{11}=\alpha_{11}/J$, $b_{12}=-\alpha_{12}/J$, $b_{21}=-\alpha_{21}/J$, and $b_{22}=\alpha_{22}/J$ where J is the determinant of the Jacobian matrix. The shear strain component γ_{xz} in the Cartesian system is

$$\gamma_{xz}=\theta_x-(w_{,\xi}\ \xi_{,x}+w_{,\eta}\ \eta_{,x}) \tag{15}$$

The consistent interpolations must now be worked out for an arbitrary orientation and shape of the element because of the presence of the terms from the inverse Jacobian. We introduce a set of covariant shear strain tensor components or covariant definitions of rotations θ_ξ and θ_η such that we can describe the Cartesian shear strain component in the following form,

$$\gamma_{xz}=(\theta_\xi-w_{,\xi})\ \xi_{,x}+(\theta_\eta-w_{,\eta})\ \eta_{,x} \tag{16}$$

where $\gamma_{\xi\xi}=(\theta_\xi-w_{,\xi})$ and $\gamma_{\eta\xi}=(\theta_\eta-w_{,\eta})$ are the covariant shear strains. The components of the shear strains in the two systems can now be readily transformed using the following relationship: $\gamma_{\xi\xi}=\alpha_{11}\gamma_{xz}+\alpha_{12}\gamma_{yz}$, $\gamma_{\eta\xi}=\alpha_{21}\gamma_{xz}+\alpha_{22}\gamma_{yz}$; $\gamma_{xz}=b_{11}\gamma_{\xi\xi}+b_{12}\gamma_{\eta\xi}$, $\gamma_{yz}=b_{21}\gamma_{\xi\xi}+b_{22}\gamma_{\eta\xi}$.

We conclude at once that consistency must now be maintained for the covariant shear strains $\gamma_{\xi\xi}$ and $\gamma_{\eta\xi}$. This means that there must be a consistent form of interpolation between θ_ξ and $w_{,\xi}$ and θ_η and $w_{,\eta}$. If the original shape functions $N_i^o(\xi, \eta)$ are used to interpolate these covariant base rotations from the nodal values of these same quantities, then it is clear from Eq. (15) that the interpolations will lead to spurious constraints. It is necessary therefore to introduce a consistent form of the interpolation so that no spurious constraints are seen. The consistent assumed shear strain field can then be represented as (see Prathap and Somashekar 1988)

$$\bar{\gamma}_{xz}=(\bar{\theta}_\xi-w_{,\xi})\ \xi_{,x}+(\bar{\theta}_\eta-w_{,\eta})\ \eta_{,x} \tag{17}$$

We interpolate $\bar{\theta}_\xi$, $\bar{\theta}_\eta$ in Eq. (17), using the values of $(\theta_\xi)_i$ and $(\theta_\eta)_i$ at the nodes and the consistently derived shape functions N_ξ^1 and N_η^1, but transform $(\theta_\xi)_i$ and $(\theta_\eta)_i$ at the nodes to the Cartesian co-ordinate definitions of the rotations $(\theta_x)_i$ and $(\theta_y)_i$ using the Jacobian transformation given earlier. This will ensure that the shear strains defined in the natural co-ordinate system continue to be consistently maintained within the element domain and across element edges so that they can vanish without generating any spurious constraints. Thus, in the case of the shear strain γ_{xz} we have

$$\begin{aligned}\bar{\gamma}_{xz}(\xi, \eta)=\sum_{i=1}^{4}\ &\{\theta_{x_i}\ [(\alpha_{11})_i(N_\xi^1)_i\ b_{11}+(\alpha_{21})_i(N_\eta^1)_i\ b_{12}]\\ &+\theta_{y_i}[(\alpha_{12})_i(N_\xi^1)_i\ b_{11}+(\alpha_{22})_i(N_\eta^1)_i\ b_{12}]-w_i[(N_{x_\xi}^o)_i\ b_{11}+(N_{x_\xi}^o)_i\ b_{12}]\}\end{aligned} \tag{18}$$

where b_{ij} are evaluated at the integrating points and α_{ij} are computed at the nodal points. Similarly, the shear strain definition for γ_{yz} can be obtained.

A note on the form of the consistently derived shape functions N_ξ^1 and N_η^1 will be in order here. Once these are derived for a specific application, i.e., a 4-node or 8-node or 9-node element

as the case can be, the description of the shear stiffness formulation given above is very general as long as the summation is done correctly over the n nodes and the appropriate original N^o functions and smoothed (N_ξ^1), (N_η^1) functions are used. We can derive N_ξ^1 and N_η^1 as follows. We need, for example, a consistent $\bar{\gamma}_{\xi\xi}$ to be derived from $\gamma_{\xi\xi}$. In (Prathap and Somashekar 1988) this was done using a variational condition of the form

$$\int\int \delta\bar{\gamma}_{\xi\xi}^T(\bar{\gamma}_{\xi\xi}-\gamma_{\xi\xi})\, d\xi\, d\eta \tag{19}$$

The element developed on this basis does not lock, passes all the patch tests prescribed for this element, is invariant to node numbering and is the simplest and most efficient 4-noded plate bending quadrilateral element known to us. A simple application of reduced or selective integration would never have satisfied the consistency requirments seen to exist in the general quadrilateral form.

5. Numerical experiments

Elements formulated using the field-consistency approach have been rigorously tested using the accepted benchmark single-element and patch tests (Prathap and Somashekar 1988, Prathap 1993, Prathap 1994) and appear to meet the various requirements expected of elements to be used for prodcution-run analysis tasks. We shall briefly review this here.

Our numerical studies here will consider the inconsistent and field-consistent versions of the element:

$I-\theta_x$ and θ_y interpolated by the original shape functions, i.e., field-and edge-inconsistent.

$C-\theta_\xi$ and θ_η interpolated by the smoothed shape functions, but transformed to θ_x and θ_y at the nodes, i.e., field- and edge-inconsistent.

These studies will confirm that the C version is the optimal element. Our subsequent tests will place particular emphasis on the effects of distortion and arbitrary orientation on this quadrilateral element (henceforth called QUAD4) in meshes in several benchmark tests.

5.1. Cantilever plate test

A cantilever plate of dimensions 100 by 100 and thickness 0.1 is modelled by two elements in the configurations A and B shown in Fig. 3. The elastic properties chosen are $E=10^5$ and $\nu=0.0$. The free edge is loaded by a bending moment distributed at nodes 5 and 6 equally as shown in the Figure. The deflections w_5 and w_6 at the nodes 5 and 6 and the bending moment resultant M_{xx} at the centroid of the second element are given in Table 2. It is clear that even with a rectangular grid, field-inconsistency (the I element) leads to very large locking effects. However, the C element is totally free of locking. The distorted Mesh B now shows that the field-inconsistent element has a significant degree of locking. However, the optimal C element is totally free of any difficulties.

5.2. Constant strain patch tests

The most frequently used patch test is a configuration of five arbitrary quadrilateral elements

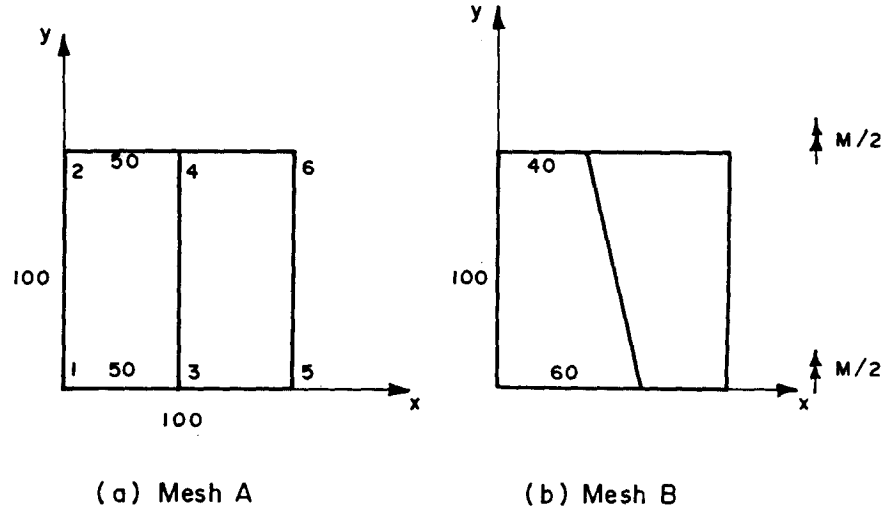

Fig. 3 Two element cantilever plate test.

Table 2 Deflections at nodes 5 and 6 and bending stress resultant M_{xx} at centroid of element 2 (Fig. 3)

Ele.	w_5		w_6		M_{xx}	
	Mesh A	Mesh B	Mesh A	Mesh B	Mesh A	Mesh B
I	0.58e-6	0.57e-6	0.58e-6	0.54e-6	0.97e-7	0.97e-7
C	0.60e-1	0.60e-1	0.60e-1	0.60e-1	1.00e-2	1.00e-2
Exact	0.60e-1				1.00e-2	

as shown in Fig. 4a. We shall consider four types of straining configurations as in the sub-sections below.

5.2.1. Constant bending strain test

A distributed edge couple of constant intensity on the right hand edge is simulated by two concentrated edge couples as shown in Fig. 4b. Version I fails this test. However, version C satisfies it exactly.

5.2.2. Constant shear strain test

A uniformly distributed edge load is simulated by two equal concentrated loads as shown in Fig. 4b. Note that the imposed conditions imply that all rotations are zero and that only pure shear is possible. No field-inconsistency problem can therefore manifest itself here and as expected, both versions I and C pass this simple test.

It is in this form that this test is used in the literature and it is clear from the present experiment that this test fails to bring out the essential nature of the inconsistency problems faced by the I version of the element. In the next sub-section, we offer a more useful patch test to highlight this feature.

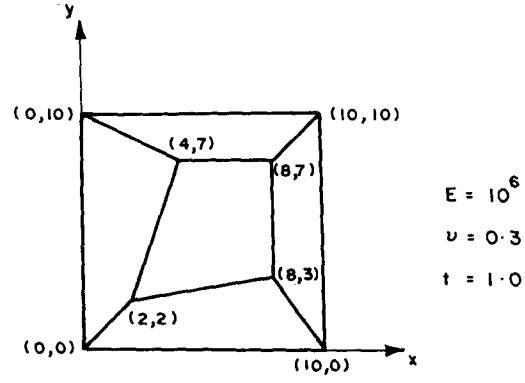

(a) Patch of elements used

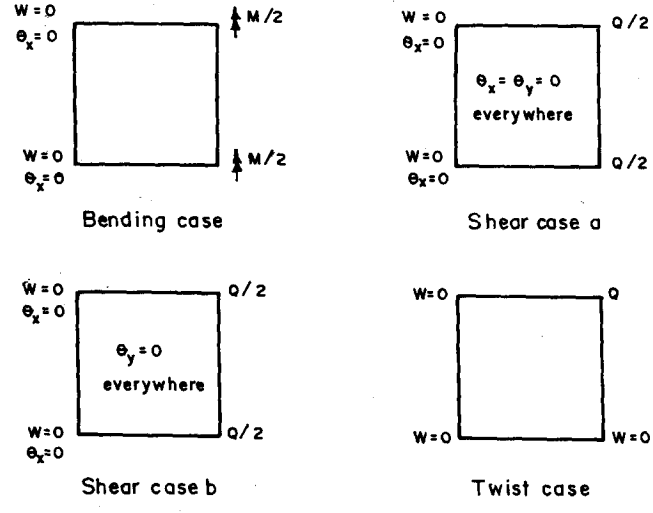

(b) Various loading cases

Fig. 4 Constant strain patch tests.

5.2.3. *Constant shear and linear bending strain test*

To understand more realistically how field-inconsistencies are induced under shearing, the shear test is repeated allowing the rotations θ_x to develop. This corresponds to a constant shear and linear bending strain patch test (Shear case b of Fig. 4). Again, only the version C is able to satisfy this patch test.

5.2.4. *Constant twisting strain test*

The plate is now supported at three corner points and is loaded by a concentrated shear force at the fourth corner (Twist case of Fig. 4b). Classical thin plate theory predicts that a pure constant state of twisting strain is developed in the patch. For a thin plate (thickness $t=0.001$ in.) only version Cφ passes this patch test.

6. Conclusions

We believe (Prathap 1993, Prathap 1994) that the field-consistency paradigm offers a complete scientific framework to understand the locking problem and also provides procedures to design efficient plate and shell elements based on first-order or higher-order plate theories. If the ambition is to be able to derive plate and shell elements in a unified and generic way from a simple set of first principles, the field-consistency principle offers a rational basis to achieve this.

References

Ahmed, S., Irons, B.M. and Zienkiewicz, O.C. (1970), "Analysis of thick and thin shell structures by curved finite elements," *Int. J. Numer. Meths. Engrg.*, **2**, 419-451.

Hughes, T.J.R., Taylor, R.L. and Kanok-Nukulchai, W. (1977), "A simple and efficient finite element for plate bending", *Int. J. Numer. Meths. Engrg.*, **11**, 1529-1543.

Mindlin, R.D. (1951), "Influence of rotary inertia and shear on flexural motion of isotropic elastic plates," *J. Appl. Mech.*, **18**, pp. 31-38.

Pawsey, S.F. and Clough, R.W. (1971), "Improved numerical integration o9f thick shell finite elements," *Int. J. Numer. Meths. Engrg.*, **3**, 575-586.

Prathap, G. (1993), *The Finite Element Method in Structural Mechanics*, Kluwer Academic Publishers, Dordrecht.

Prathap, G. (1994), "The displacement-type finite element approach-form art to science", *Prog. Aerospace Sci.*, Vol. 30, 295-405.

Prathap, G. and Somashekar, B.R. (1988), "Field- and edge-consistency synthesis of a 4-noded quadrilateral plate bending element," *Int. J. Numer. Meths. Engrg.*, **26**, 1693-1708.

Stolarski, H. and Belytschko, T. (1982), "Membrane locking and reduced integration for curved elements", *J. Appl. Mech.* **49**, 172-178.

Zienkiewicz, O.C., Taylor, R.L. and Too, J.M. (1971), "Reduced integration technique in general analysis of plates and shells," *Int. J. Numer. Meths. Engrg.*, **3**, 275-290.